

Multi-class Cervical Cancer Classification using Transfer Learning-based Optimized SE-ResNet152 model in Pap Smear Whole Slide Images

Original Scientific Paper

Krishna Prasad Battula

School of Computer Science and Engineering,
VIT-AP University, Amaravathi, Andhra Pradesh, India.
krishnaprasadbattula706@gmail.com

B. Sai Chandana

School of Computer Science and Engineering,
VIT-AP University, Amaravathi, Andhra Pradesh, India.
saichandanas869@gmail.com

Abstract – Among the main factors contributing to death globally is cervical cancer, regardless of whether it can be avoided and treated if the afflicted tissues are removed early. Cervical screening programs must be made accessible to everyone and effectively, which is a difficult task that necessitates, among other things, identifying the population's most vulnerable members. Therefore, we present an effective deep-learning method for classifying the multi-class cervical cancer disease using Pap smear images in this research. The transfer learning-based optimized SE-ResNet152 model is used for effective multi-class Pap smear image classification. The reliable significant image features are accurately extracted by the proposed network model. The network's hyper-parameters are optimized using the Deer Hunting Optimization (DHO) algorithm. Five SIPaKMeD dataset categories and six CRIC dataset categories constitute the 11 classes for cervical cancer diseases. A Pap smear image dataset with 8838 images and various class distributions is used to evaluate the proposed method. The introduction of the cost-sensitive loss function throughout the classifier's learning process rectifies the dataset's imbalance. When compared to prior existing approaches on multi-class Pap smear image classification, 99.68% accuracy, 98.82% precision, 97.86% recall, and 98.64% F1-Score are achieved by the proposed method on the test set. For automated preliminary diagnosis of cervical cancer diseases, the proposed method produces better identification results in hospitals and cervical cancer clinics due to the positive classification results.

Keywords: Cervical cancer; affected tissues; image classification; Pap smear images; and loss function

1. INTRODUCTION

The fourth most prevalent cancer in women worldwide and the seventh most common overall is cervical cancer [1]. Cervical cancer is primarily brought on by early sexual activity, poor menstrual hygiene, oral contraceptive use, smoking, a weakened immune system, early pregnancy, and sexual activity with several partners [2, 3].

The diagnosis of cervical cancers frequently uses cytopathology screening [4]. The doctor uses the brushes to extract cells from a patient's cervix during a cervical cytopathological examination, and the exfoliated cells are then placed on a glass slide [5]. If a tumor is malignant, cytopathologists examine it under a microscope to confirm this [6]. Each slide contains thousands of cells, though. As a result, inspection manually is complicated, and specialists are vulnerable to mistakes. So, a better solution is required for this issue [7, 8].

This issue is resolved by developing automatic computer-aided diagnosis (CAD) systems. Rapid and reliable pap slide analysis is possible with CAD [9]. The bedrock of early CAD was traditional machine learning and image processing techniques; the manually created features may produce poor categorization results [10, 11]. Deep learning technology has made advancements recently in several.

Sectors, including natural language processing (NLP), medical imaging, computer vision, and others [12]. Deep learning is a new type of machine learning that can automatically learn characteristics for classification. Yet, many labeled data sets are needed to train a deep learning model [13, 14]. A popular deep learning network is a Convolutional Neural Network (CNN), frequently utilized in image detection, classification, and segmentation [15, 16].

The research presented in this research is limited to various cervical cancer cases, which are challenging to categorize compared to earlier methods [17]. The highest-performing CNN model is initially chosen based on a thorough experiment [18]. Finally, it assesses the combination of performance enhancements, including optimizer selection and image enhancement [19, 20]. The generalization and high performance of DL approaches for classification are incorporated into the proposed method. It is suggested to use transfer learning to classify Pap smear images into several types of cervical cancer disorders using the deep learning-based hybrid network model.

The main contributions of the research are,

- Initially, image pre-processing is used to enhance the quality of image data by avoiding unwanted distortions. Mathematical morphology operations are used for image enhancement to increase classification performance.
- After completing a pre-processing phase, the transfer learning-based optimized SE-ResNet152 model is used for effective classification. The proposed model effectively classifies the Pap smear images into 11 classes using CRIC and SIPaKMeD dataset images.
- The reliable disease image features are successfully extracted by the proposed network model for effective classification results. The CNN hyperparameters are optimized using the DHO optimization methods, which produce results with greater accuracy in diagnosing multiple diseases.
- On the publicly available datasets, the proposed approach is assessed. The experiments are performed on the Python platform.
- The proposed approach outperforms the state efficiency concerning all other approaches, according to the experimental data.

The work is organized as follows. Part 2 of the paper discusses cutting-edge methods for classifying Pap smear images. The deep learning-based models for Pap smear image categorization that have been proposed are described in Section 3. We also cover the databases used for the experimental assessment of the effectiveness and performance of the proposed approach. Section 4 discusses the evaluation parameters and findings. Finally, the research is concluded in Section 5.

2. LITERATURE SURVEY

In this section, we review some existing deep-learning techniques for diagnoses of cervical cancer classification using Pap smear images. Desiani et al. [21] proposed the Bi-path architecture, which combined image segmentation and classification. The multiple image processing stages are proposed in this paper, including image enhancement, segmentation, and classification for recognizing and identifying cervical cancer feature on the Pap-smear images. The image quality is improved by using enhancement approaches like Nor-

malization, CLAHE, and Adaptive Gamma Correction before segmentation. Segmentation using the CNN architecture is the first step. Using the KNN and ANN algorithms to segment data yields the second path, a classification process.

Yaman et al. [22] have suggested an approach for the early identification of cervical cancer based on an exemplar pyramid structure. This structure is mainly used for feature extraction. The research aims to categorize cervical cells in pap-smear images to detect malignancy. The model pyramid deep feature generator was created using the SIPaKMeD and Mendeley Liquid-Based Cytology (LBC) datasets. The suggested feature generator generates 21,000 features using transfer learning-based feature extraction from DarkNet19 or DarkNet53 networks in an example pyramid structure. Using Neighborhood Component Analysis (NCA), The Support Vector Machine (SVM) method classifies the 1000 features NCA chose.

A simple yet efficient ensemble method is proposed by Diniz et al. [23] for improving the classification task. To address the imbalance in the dataset, a data augmentation mechanism is applied. This research presents classification analyses of two, three, and six classes. Several pap smear image classification tasks are performed using the deep learning-based EfficientNet model.

In their proposal [24], Alquran et al. used the unique Cervical Net and Shuffle Net to develop a computer-aided cervical cancer diagnosis method. 544 resulting characteristics are retrieved automatically using pre-trained CNN fused with a new Cervical Net structure. PCA is used to reduce dimension and choose the most crucial features.

Win et al. [25] created a new computer-assisted cervical cancer screening system. The cervical cancer screening system depends on the analysis of Pap smear images. The cervical cancer screening process includes four fundamental phases. In segmenting cells, nuclei were found using an iterative shape-based technique. From the regions of segmented nuclei and cytoplasm, three significant features were extracted during the features extraction step. The approach for selecting features, RF (random forest), was employed. Bagging ensemble classifiers, such as bagged trees, boosted trees, KNN, SVM, and LD, were used to integrate the output of five classifiers in classification.

A segmentation and classification system for Pap smear images was developed by Hussain et al. [26]. The Unet model is proposed for this classification. In this model, a fully convolutional layer, densely connected blocks, and residual blocks are connected in the Unet architecture. To guarantee feature reuse-ability, the number of convolutional layers in the conventional Unet has been replaced by densely connected blocks. Residual blocks have also been included to speed up network convergence. A stacked auto-encoder-based shape representation learning model precedes the suggested approach to improve the reliability of the entire network.

The multi-class classification of cervical cells using Whole Slide Imaging (WSI) with optimal feature extraction was proposed by Bhatt et al. [27]. Conv-Net with Transfer Learning approach actualization substantiates significant Metamorphic pre- and post-neoplastic lesions diagnosis. Conv-Net with Transfer Learning approach actualization substantiates significant Metamorphic pre- and post-neoplastic lesions diagnosis. The retrieved morphological cell features can be carried over by the model recursively to future Neural Network layers for illusive learning.

3. PROPOSED METHODOLOGY

Evaluating various classification improvement strategies through an experimental process to improve the performance of automated multi-class cervical cancer

classification and detection is the major concept of the proposed model. The 11 classes of cervical cancer diseases (multi-class classification) are classified in this research as ASC-H, ASC-US, SCC, HSIL, LSIL, NILM, Dyskeratotic, Koilocytotic, Metaplastic, Parabasal, and Superficial-Intermediate. The combination of CRIC and SIPaKMeD dataset images is used to analyze the proposed model using Pap smear images. The Data were obtained from publicly available open sources. For image pre-processing, contrast enhancement is accomplished by applying mathematical morphology processes in the Pap smear images. Then, a transfer learning-based optimized SE-ResNet152 model for classifying multiple cervical cancer diseases was proposed. The hypermeters are optimized by the DHO optimizer. The schematic diagram of the proposed method is given in Fig. 1.

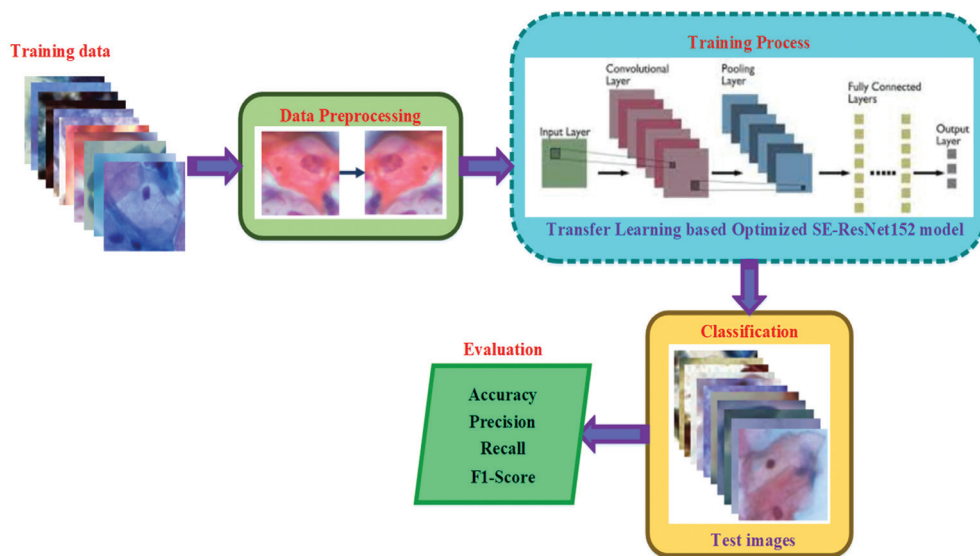


Fig. 1. Schematic diagram of the proposed methodology

3.1. IMAGE PRE-PROCESSING

Mathematical morphology has been applied to enhance contrast in the Pap smear images. The structural values of objects are the basis for how mathematical morphology methods operate. These techniques leverage interactions between classes and basic mathematical concepts to identify the components of an image and clarify spatial relationships. Two different data sets are used as input for morphological operators. In morphological operators, equations 1 and 2 define the erosion and dilation operators. This process represents the gray-level image matrix I and defines the structural element.

$$I \ominus S = \min_{m,n} \{I(x+m, y+n) - S(m,n)\} \quad (1)$$

$$I \oplus S = \max_{m,n} \{I(x-m, y-n) + S(m,n)\} \quad (2)$$

In the erosion process, the size of the objects is reduced. Minimal information from that image is also eliminated by this erosion process. In other words, image gap size reduces, and object size rises when the

dilation operator is used in reverse. As a result, the closing operator behaves similarly to applying the dilation and erosion operations to the same image in equation 3, while the opening operator acts in equation 3.

$$I \circ S = (I \ominus S) \oplus S \quad (3)$$

$$I \bullet S = (I \oplus S) \ominus S \quad (4)$$

Tiny gaps are filled in by the opening operator, who also eliminates bad relationships between artifacts and small amounts of information. Nonetheless, disk-shaped SEs are utilized more commonly than other masks for medical pictures. The size and shape of a SE are typically chosen at random.

3.2. FEATURE EXTRACTION BASED ON TRANSFER LEARNING

Extracting cervical image characteristics is a prerequisite for the multi-class classification of cervical cancer. The classifier's classification performances are directly impacted by the effectiveness of feature extraction. Traditional

deep-learning classification applications sometimes call for expensive computing resources and big datasets for training from scratch. For extracting the significant image features in this research, we utilized Modifying SE-ResNet152 models that were trained to decrease the reliance on the amount of data and accelerate model training. Textural, statistical, wavelet, and morphological features of the Pap smear images are extracted to improve the classification performance. The weights and parameters are updated by training the modified SE-ResNet152 model. For multi-class classification of cervical cancer, high-quality features of the image are extracted by fine-tuning the transfer learning model.

3.2.1. ResNet

The residual adding unit is more useful for addressing the challenge of the deeper neural network, which solves the vanishing gradients problem of the network. An entirely new trend in image recognition has been launched by ResNet. To teach desirable features, appropriate depth is still essential. The stacked layers might enhance the "levels" of features (depth). The cervical image features are effectively extracted using 152-layer ResNet (ResNet152), which increases the obtained accuracy from the increased depth and uses fine-grained and small-scale features of the Pap smear image dataset.

The residual function is represented as

$$Q(z) = P(z) - z \quad (5)$$

The parameter function is represented by P , which was directly learned through training, x is the input, and the residual function is denoted as $Q(z)$. It will be challenging to train deep networks if "simple" layers can directly fit a possible identity mapping function $P(z)=z$. The residual network is easier to optimize and converges more quickly when $P(z)=Q(z)+z$ transformed into a residual function. Feature extraction with more extraordinary expression ability is possible by slightly increasing the network's depth.

3.2.2. SENet

The basis of SENet is its feature recalibration method, which allows it to emphasize insightful data while suppressing less helpful ones selectively. This mechanism automatically determines the value of each feature channel. Squeeze-and-excitation (SE) blocks make up the SENet architecture. The model's sensitivity to channel properties can be increased, and its performance can be significantly improved by incorporating the SE block into the current network layout. The SE-ResNet152 model's organizational structure is depicted in a schematic in Figure 5.

In ResNet152, the SE block is included for creating high-quality Pap smear image features considering the slight visual variations between various cervical cancer illnesses. Combining 1×1 and 3×3 convolutions, the residual module, as seen in Figure. 2, lowers the parameters. The dynamic relationship between channels is fitted by

connecting two fully connected (FC) layers with a bottleneck structure, and the input image's global features are obtained by enabling global pooling in the network model. The first FC layer performs dimensionality reduction, followed by activation using a ReLU and restoration of the original dimension by the last FC layer. A sigmoid operation yields the normalized weights. The entire activity shown in the image can be viewed as an attention mechanism that aims to strengthen the network's capacity for representation. Based on the abovementioned processes, the proposed transfer learning-based optimized SE-ResNet152 model performance is improved for effective classification.

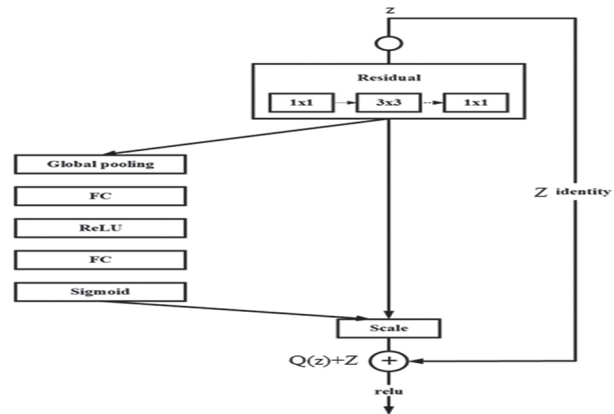


Fig. 2. SE-ResNet152 model structure example diagram

3.2.3. Loss function

Due to data imbalance, classifiers will produce poor classification results, particularly for classifications with few samples. For enhancing a loss function, the accuracy of cervical cancer identification can be significantly increased by applying a re-weighting technique.

$$CB(p, y) = \frac{1}{E_{n_y}} L(p, y) = \frac{1 - \beta}{1 - \beta^{n_y}} L(p, y) \quad (6)$$

Where n_y the ground-truth class's total sample is given by S_y , where x is the sample, the model's probability distribution $P=[p_1, p_2, \dots, p_c]$ $p_i \in [0,1]$ $L(P, y)$ is defined by the loss function. The class-balanced term is adjusted by the hyperparameter β .

The focal loss function is:

$$Focal\ Loss(z, y) = - \sum_{i=1}^c \left(1 - p_i^t\right)^{\gamma} \log(p_i^t) \quad (7)$$

It is possible to express the class-balanced focal loss as

$$CBfl(z, y) = - \frac{1 - \beta}{1 - \beta^{n_y}} \sum_{i=1}^c \left(1 - p_i^t\right)^{\gamma} \log(p_i^t) \quad (8)$$

We define z_i^t as

$$z_i^t = \begin{cases} z_i, & \text{if } i = y \\ -z_i, & \text{ow} \end{cases} \quad (9)$$

The model's output is $z=[z_1, z_2, \dots, z_c]^T$ where the overall number of classes is indicated by C .

3.3. DEER HUNTING OPTIMIZATION (DHO) ALGORITHM

The way humans hunted deer served as an inspiration for the traditional DHOA. Finding the person's optimal or most productive deer hunting stance is the primary goal of traditional DHOA. Deers, also called a buck, have specific characteristics that allow them to protect themselves from predators or hunters. The distinguishing features include the capacity to detect ultrahigh-frequency noises, an excellent sense of smell, and exceptional vision.

Testing findings that demonstrate overfitting values, like in the case of the combined dataset, requires the hyperparameter tuning process. The best value is produced by the data training detection rate. Loss function values, activation function, initialization weights, learning rate value, and the number of layers and neurons must all be examined to establish the ideal model. These network model parameters are optimized for improving the accuracy and precision of the classification of Pap smear images. In each layer, the system's complexity is influenced by the number of neurons. The training and response times often rise as the number of neurons increases. Capacity in the multilayer model is controlled by the number of neurons in each layer. Automated feature engineering's complicated data representation makes adding layers beneficial to learning. Depending on how complicated the dataset is, layer addition can increase accuracy. The conventional DHOA is composed of four processes in terms of mathematics.

Phase 1: Initializing the population: Equation (10) creates the hunter population. The population of hunters and the average number of hunters are represented as H and S .

$$H = \{H_1, H_2, \dots, H_S\} ; 1 < r \leq se \quad (10)$$

Phase 2: The wind initialization and position angle: Establishing the location and wind angle is the first step in determining the ideal position for creatures to hunt deer. The wind angle is computed by Equation (11), while the position angle is computed by Equation (12). A number at random between [0, 1] is l , the present iteration is k , ϕ represents the wind angle, and the position angle is represented by θ notation.

$$\phi_k = 2\pi l \quad (11)$$

$$\theta_k = \phi + \pi \quad (12)$$

Phase 3: Propagation of position

The fitness function determines the optimal space, the area closest to the most optimal solution. Two roles are typically described: successor (Hsuccessor) and leader (Hlead). The propagation process makes use of the leader's position. Everyone in the community works hard to land the best positions once they are identified, and then

updating the job description starts. The equation provides the hunter's encircling formula's empirical formula (13)

$$H_{k+1} = H^{lead} - M.c. | R \times H^{lead} - H_k | \quad (13)$$

In Eq (14), the current position of the hunters is represented H_k , and the upgraded position of the predators is described H_{k+1} in the following procedure. In contrast, the random number c , which ranges from 0 to 2 for considering the wind angle, is represented. This uses the random integer rd , which ranges from 0 to 1. It K_{max} gives the maximum number of iterations, and the coefficient vectors (M) are calculated below the equation,

$$M = \frac{1}{4} \log \left(K + \frac{1}{K_{max}} \right) a \quad (14)$$

$$R = 2 \cdot rd \quad (15)$$

Using position angle as a basis for propagation: During the hunter's location improvement process, this is accomplished by improving the search space by considering the position angle. The position angle is determined to increase the effectiveness of the deer hunting activity. Moreover, a parameter ds_k is derived from the difference between the visualization and wind angles for improving the position angle, as given in equation (16). Equation (17) determines the prey's vision vs_k angle.

$$ds_k = \phi_k - vs_k \quad (16)$$

$$vs_k = \Pi / 8 \times rad \quad (17)$$

Equation (18) updates the position angle, and equation (19) upgrades the hunter's location by accounting for the position angle.

$$\theta_{k+1} = \theta_k + ds_k \quad (18)$$

$$H_{k+1} = H^{lead} - c. | \cos(\omega) \times H^{lead} - H_k | \quad (19)$$

The propagation process for the successor position is as follows: The encircling procedure is used to alter the vector R during the exploring stage. The vector R -value is considered smaller than one when evaluating the random search in its beginning position. Equation illustrates how updating the hunter's position is based on the successor's location (20). The search agent is chosen probabilistically if the vector R -value is less than 1; else, the best solution for improving the positions of the search agents is generated.

$$H_{k+1} = H^{successor} - M.c. | R \times R^{successor} - R_k | \quad (20)$$

Phase 4: End procedure: This is the last stage of the DHOA algorithm. The position updating procedure is repeated until the ideal location is discovered.

4. RESULT AND DISCUSSION

This section examines the many performance measurements used to assess the method, compares the proposed method to current state-of-the-art procedures, and makes comparisons. Using Python, the experimental evaluation is carried out. Each model's input requirements are fulfilled by standardizing the

size and resolution of the images. Several cervical cancer diseases are classified using the transfer learning-based optimized SE-ResNet152.

4.1. DATASETS

4.1.1. CRIC

400 conventional Pap smear images from the CRIC collection, including 11534 cells identified manually. There are six different types of images: negative for intraepithelial lesion or malignancy (NILM); low-grade squamous intraepithelial lesion (LSIL); high-grade squamous intraepithelial lesion (HSIL); squamous cell carcinoma (SCC); possibly non-neoplastic (ASC-US); atypical squamous cells of

undetermined significance; cannot exclude a high-grade lesion (ASC-H); and atypical squamous cells. Including 4789 images of cervical cells that have been separated, this paper exclusively uses cropped images. Fig. 3 displays a few examples of images of the CRIC dataset.

4.1.2. SIPaKMeD

Cervical cell image classification tasks are possible using the SIPaKMeD dataset. The images collected by the camera and cropped into 4049 cervical cell images help compensate for this dataset. These images are divided into five categories: superficial intermediate, parabasal, metaplastic, koilocytotic, and dyskeratotic. Fig. 4 shows some example images of the SIPaKMeD dataset.

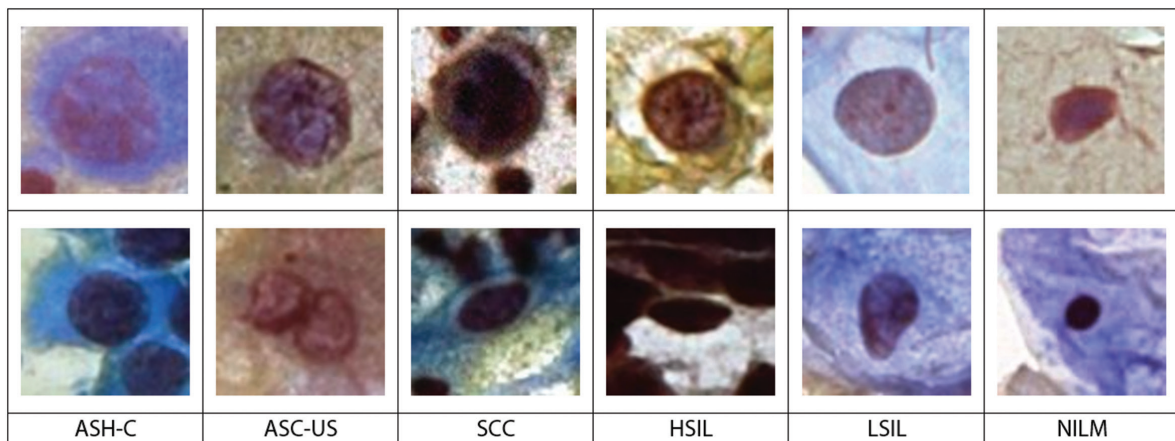


Fig. 3. Sample images of a CRIC dataset

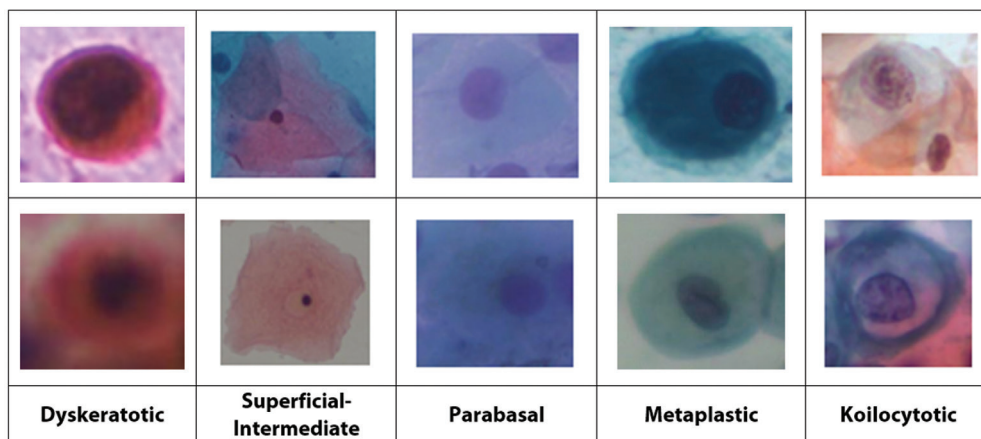


Fig. 4. SIPaKMeD dataset images

4.1.3. combination of datasets used for analysis

We integrated the CRIC and SIPaKMeD datasets for this investigation. This integration of dataset images is used for experiment analysis. As a result, we obtained 11 categories, comprising the CRIC dataset's six categories and the SIPaKMeD dataset's five categories. There are 8838 images in this combined dataset. For the test, validation, and training sets, we chose 20%, 20%, and 60%, respectively, randomly from each class of images. Table 1 displays the data configurations.

Table 1. The combined dataset's data settings

Class/Dataset	Test	Validation	Train	Total
Superficial-Intermediate	166	166	499	831
Parabasal	157	157	473	787
Metaplastic	158	159	476	793
Koilocytotic	165	165	495	825
Dyskeratotic	162	163	488	813
SLIM	518	172	172	862
LSIL	163	164	491	818

HSIL	174	175	525	874
SCC	137	137	413	687
ASC-US	148	148	446	742
ASC-H	161	161	484	806
Total	1763	1767	5308	8838

4.2. EXPERIMENTAL SETTINGS

This research experiment was performed on a local computer running Windows 10 and equipped with 32 GB of RAM. The Pytorch version we are using is 1.8.0, and we are using the Python programming language. Using the Adam optimizer's hyperparameter configuration for training the proposed network model is shown in Table 2.

Table 2. Hyperparameter settings for network training

Parameter	Value
Momentum	0.9
Decay	10-5
Learning rate	0.0002
Batch size	16
Epoch	100

4.3. EVALUATION METHODS

Calculations are made to assess the performance of the suggested model using precision, recall, F1-Score, and accuracy. The number of precisely anticipated positive samples is called True Positive (TP). There are exactly as many True Negative (TN) as predicted negative samples. False Positives (FP) are negative sample range that was expected to be positive. Moreover, False Negatives (FN) are samples that were positive but were later found to be negative. Precision is the percentage of TP in all correct predictions. The proportion of anticipated positive samples to all positive sample counts is known as a recall. A specific measure of precision and recall is the F1-Score. The proportion of correctly predicted occurrences to all occurrences is known as accuracy. The performance metrics are described as follows.

$$Accuracy = \frac{TP + TN}{TP + TN + FP + FN} \quad (21)$$

$$precision (p) = \frac{TP}{TP + FP} \quad (22)$$

$$Recall (R) = \frac{TP}{TP + FN} \quad (23)$$

$$F1-Score = 2 \times \frac{p \times R}{p + R} \quad (24)$$

4.4. EXPERIMENTAL RESULTS AND ANALYSIS

The proposed model's performance is assessed throughout the test and validation phases using accuracy, F1-Score, recall, and precision calculations, as illustrated in Fig. 5. The proposed model obtains 98.95% of precision, 98.23% of recall, 98.93% of F1-Score, and

99.89% of accuracy on the validation set from the experiment results. The proposed model obtains 98.82% of precision, 97.86% of recall, 98.64% of F1-Score, and 99.68% of accuracy on the test set. The proposed model's excellent generalizability is demonstrated by the little performance difference we acquired between the validation set and the test set. The performance of the suggested model outperforms the existing approaches and yields excellent outcomes.

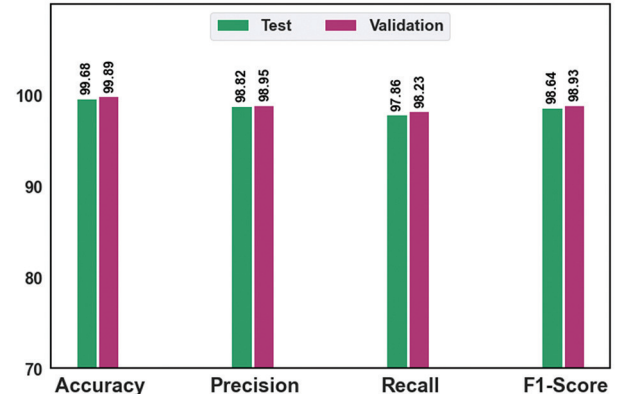
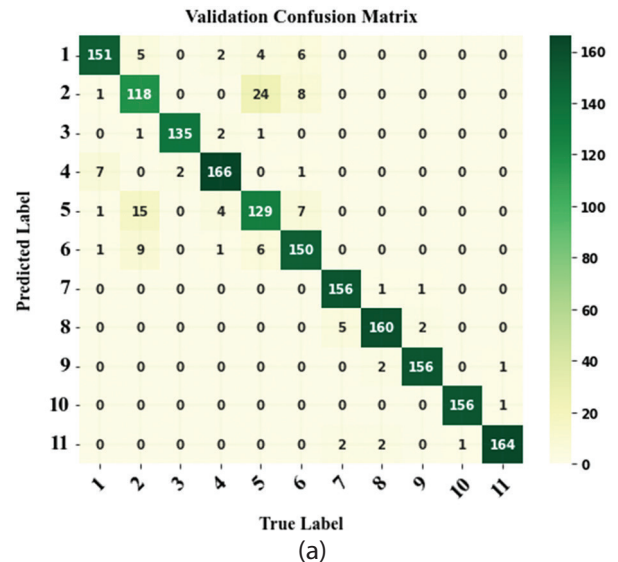


Fig. 5. The performance of the proposed transfer learning-based optimized SE-ResNet152 model

For validation and testing, Fig. 6 displays the confusion matrices using the proposed approach. The entire classification results are accurate, as seen in the validation confusion matrix. The second category's fifteen images are divided into the fifth and sixth categories, respectively, while nine are placed in the second category. The second category contains twenty-four of the five images from the fifth category. In the test confusion matrix, the result is much the same. In the sixth category, nine images from the second and twenty-one from the fifth categories were incorrectly assigned. In the fifth category, 11 images are incorrectly categorized into the sixth category, and 22 are incorrectly classified into the second category. The eighth category was incorrectly assigned to 11 images in the seventh category.



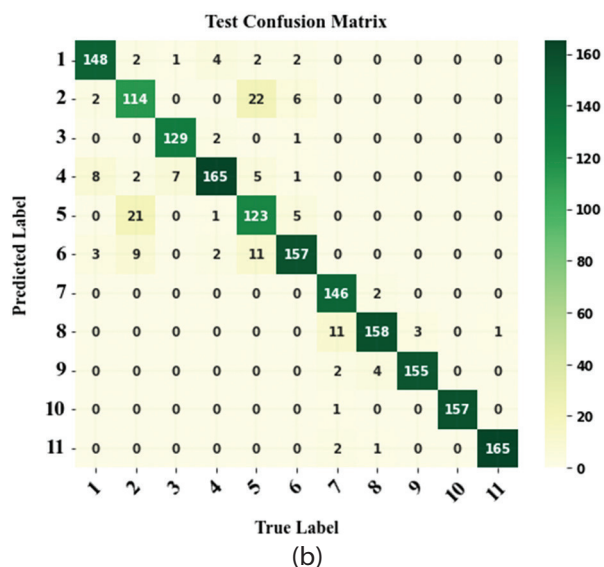


Fig. 6. The proposed model's confusion matrices for both (a) validation and (b) testing

These eleven categories are broken down into abnormal types for the first, third, fourth, seventh, and eighth categories. The proposed approach has a greater level of classification accuracy for abnormal types. Because

Table 3. Comparative analysis of proposed approach and state-of-the-art approaches

References	Year	Classes	Dataset	Method	Accuracy (%)
Win et al. [25]	2020	2 classes	SIPaKMeD dataset	Bagged trees, boosted trees, KNN, SVM, and significant voting	98.27
Dhawan et al. [28]	2021	3 classes	Kaggle dataset	InceptionV3	96.1
Kanphade and Mulmule [29]	2022	-	Benchmark database	MLP with three kernels and SVM	97.14
Alquran et al. [30]	2022	7 classes	Herlev dataset	DL and cascading SVM	92
Yaman and Tuncer [22]	2022	2 classes	SIPaKMeD	SVM	98.26
			Mendeley		99.47
Proposed Model		11 classes	CRIC dataset	Transfer learning-based optimized SE-ResNet152	99.68

Yaman and Tuncer et al. [22] proposed the SVM model for pap smear image classification, it classifies two class images, and the SVM method achieves 98.26% accuracy for the SIPaKMeD dataset and 99.47% for the Mendeley dataset. Alquran et al. [30] presented a DL and cascading SVM approach to cervical cancer classification, and it classifies multiple cervical cancer diseases with an overall accuracy of 92% using the Herlev dataset. Dhawan et al. [28] used InceptionV3 to inculcate the batch normalization layer along with every activity layer and obtained an accuracy of 96.1% for cervical cancer classification. Mulmule and Kanphade [29] introduce SVM and MLP approaches, achieving 97.14% accuracy. Win et al. [25] utilize bagged trees, boosted trees, KNN, SVM, and major voting models to classify multi-class Pap smear images, achieving an accuracy of 98.27%. While compared to the prior deep learning models, the proposed transfer learning-based optimized SE-ResNet152 model achieves better results and effectively classifies the multiple cervical cancer dis-

ease using the CRIC dataset Pap smear image dataset. The proposed transfer learning-based optimized SE-ResNet152 model has the main benefit of preventing overfitting and having no negative effects on network performance due to the classification and segmentation process.

4.5. COMPUTATIONAL TIME

The proposed network model is trained using 100 epochs in this experiment, and the size of the model parameters is around 120 MB. The training period is 1.3 hours long and consists of 5308 training images. Each training epoch lasts for around 82 seconds. Despite the lengthy training phase, the test lasts only 31 seconds. Each test image takes around 0.018 seconds to complete, totaling 1763 test images.

4.6. COMPARISON RESULTS

We compare the categorization outcomes of our suggested model with outcomes from previous research using Pap smear images in this section. The comprehensive analysis of the proposed transfer learning-based optimized SE-ResNet152 model in terms of accuracy is performed with the most advanced classifiers available, mentioned in Table 3.

The proposed approach provides a classification of 11 cervical cancer diseases based on Pap smear images using the largest dataset of images ever used. It is the more effective system that does so. The proposed CNN architecture has a high classification rate compared to previous methods.

The recent machine learning-based techniques like SVM, decision tree, K-means clustering, and Genetic algorithms produce better results on multi-class pap smear image classification. However, it still has a lot of limitations, including (i) Cannot separate overlapping cells, (ii) overfitting in case of many attributes, (iii) complex and time-consuming, (iv) usually detects only

round shapes, (v) the classification accuracy is low, (v1) challenging to obtain optimal parameters for nonlinear data and training is slow. These problems are solved by our proposed transfer learning-based optimized SE-ResNet152 model.

In the proposed transfer learning-based optimized SE-ResNet152 model, the effective significant related features of the image are extracted efficiently for improving the classification performance. In image classification, training deep neural networks from scratch on large datasets can be computationally expensive and time-consuming. Our transfer learning-based optimized SE-ResNet152 model helps overcome this challenge by starting with a pre-trained model that has already learned lower-level features, allowing the fine-tuning process to converge faster and with fewer training samples. There may be other options in many real-world scenarios than collecting and annotating a large dataset for a specific task. Our proposed transfer learning-based model allows the use of smaller datasets by leveraging the knowledge acquired from a larger dataset during pre-training. This leads to better generalization and improved performance, even with limited labeled data.

4.7. ADVANTAGES OF THE PROPOSED APPROACH

The suggested model successfully extrapolates characteristics that describe the inter-scale heterogeneity of the diseases, enhancing classification performance. For classifying Pap smear images, the proposed method performs better than the existing methods; the proposed method achieves a 99.68% accuracy, 98.82% precision, 97.86% recall, and 98.64% F1-Score. As a result of the proposed model's impressive classification accuracy, cervical cancer disorders are automatically detected and pre-screened.

4.8. DISADVANTAGES OF THE PROPOSED APPROACH

The experimental results indicate that the proposed approach can classify multiple cervical cancer diseases. However, this field still requires more research to be done. The proposed approach offered greater accuracy when compared to the other models. Here, a few of the limitations are highlighted,

- The proposed method's drawback is that concatenated features' dimensions are more significant. It may be possible to minimize this set of features in the future by using a feature reduction strategy.
- Transfer learning models tend to be complex, with many layers and parameters. We will use hybrid hyperparameter optimization for effective parameter tuning and reduction.

5. CONCLUSION

The transfer learning-based optimized SE-ResNet152 model is a deep learning-based framework proposed for cervical cell categorization tasks in this paper. Using a huge dataset of images, the proposed model was also tested and trained. For noise removal and contrast enhancement, these images are pre-processed initially. The transfer learning-based SE-ResNet152 model with a DHO optimizer is used to analyze this image dataset to classify and identify the multiple cervical cancer diseases (11 classes). The distinction between Pap smear images with very high accuracy, sensitivity, and sensitivity with a considerable decrease in time taken for detection and epochs according to the proposed model results. The proposed transfer learning-based optimized SE-ResNet152 model effectively classifies the Pap smear images with an overall accuracy of 99.68%. Experiment results on segmentation benchmarks demonstrated that the proposed model outperformed several existing deep-learning network models by a large margin and gained comparable performance with other typical cervical cancer classification approaches.

To enhance the efficiency of the proposed approach, we will attempt to employ different new model configurations in the future. Along with updating the module structure, improving the capacity to extract features is possible. In the future, different data pre-processing methods, including random cropping and color jittering, will be used to enhance the model's generalization abilities.

6. REFERENCE

- [1] W. William, A. Ware, A. H. Basaza-Ejiri, J. Obungoloch, "A pap-smear analysis tool (PAT) for the detection of cervical cancer from pap-smear images", *Biomedical engineering online*, Vol. 18, 2019, pp. 1-22.
- [2] P. Wang, J. Wang, Y. Li, L. Li, H. Zhang, "Adaptive pruning of transfer learned deep convolutional neural network for classification of cervical pap smear images", *IEEE Access*, Vol. 8, 2020, pp. 50674-50683.
- [3] E. Hussain, L.B. Mahanta, C. R. Das, R. K. Talukdar, "A comprehensive study on the multi-class cervical cancer diagnostic prediction on pap smear images using a fusion-based decision from ensemble deep convolutional neural network", *Tissue and Cell*, Vol. 65, 2020, p. 101347.
- [4] D. Riana, Y. Ramdhani, T. P. Rizki, A. N. Hidayanto, "Improving hierarchical decision approach for single image classification of pap smear", *Inter-*

- national Journal of Electrical and Computer Engineering, Vol. 8, No. 6, 2018, p. 5415.
- [5] W. Liu et al. "CVM-Cervix: A hybrid cervical Pap-smear image classification framework using CNN, visual transformer and multilayer perceptron", *Pattern Recognition*, Vol. 130, 2022, p. 108829.
- [6] M. A. Mohammed, F. Abdurahman, Y. A. Ayalew, "Single-cell conventional pap smear image classification using pre-trained deep neural network architectures", *BMC Biomedical Engineering*, Vol. 3, No. 1, 2021, p. 11.
- [7] S. Fekri-Ershad, "Pap smear classification using combination of global significant value, texture statistical features and time series features", *Multimedia Tools and Applications*, Vol. 78, No. 22, 2019, pp. 31121-31136.
- [8] R. Gupta, A. Sarwar, V. Sharma, "Screening of cervical cancer by artificial intelligence based analysis of digitized papanicolaou-smear images", *International Journal of Contemporary Medical Research*, Vol. 4, No. 5, 2017, pp. 2454-7379.
- [9] D. Selvathi, W. R. Sharmila, P. S. Sankari, "Advanced computational intelligence techniques based computer aided diagnosis system for cervical cancer detection using pap smear images", *Classification in BioApps: Automation of Decision Making*, *Lecture Notes in Computational Vision and Biomechanics*, Vol. 26, Springer, Cham., 2018, pp. 295-322.
- [10] V. Kumararaja, K. Deepa, "Pap smear image classification to predict urinary cancer using artificial neural networks", *Annals of the Romanian Society for Cell Biology*, Vol. 25, No. 2, 2021, pp. 1092-1098.
- [11] C. W. Wang et al. "Artificial intelligence-assisted fast screening cervical high grade squamous intraepithelial lesion and squamous cell carcinoma diagnosis and treatment planning", *Scientific Reports*, Vol. 11, No. 1, 2021, p. 16244.
- [12] P. V. Mulmule, R. D. Kanphade, D. M. Dhane, "Artificial intelligence-assisted cervical dysplasia detection using papanicolaou smear images", *The Visual Computer*, Vol. 39, 2022, pp. 1-12.
- [13] P. Wang, L. Wang, Y. Li, Q. Song, S. Lv, X. Hu, "Automatic cell nuclei segmentation and classification of cervical Pap smear images", *Biomedical Signal Processing and Control*, Vol. 48, 2019, pp. 93-103.
- [14] Y. R. Park, Y. J. Kim, W. Ju, K. Nam, S. Kim, K. G. Kim, "Comparison of machine and deep learning for the classification of cervical cancer based on cervicography images", *Scientific Reports*, Vol. 11, No. 1, 2021, pp. 1-11.
- [15] B. Nithya, V. Ilango, "Evaluation of machine learning based optimized feature selection approaches and classification methods for cervical cancer prediction", *SN Applied Sciences*, Vol. 1, 2019, pp. 1-16.
- [16] H. Chen et al. "CytoBrain: cervical cancer screening system based on deep learning technology", *Journal of Computer Science and Technology*, Vol. 36, 2021, pp. 347-360.
- [17] V. Sellamuthu Palanisamy, R. K. Athiappan, T. Nagalingam, "Pap smear based cervical cancer detection using residual neural networks deep learning architecture", *Concurrency and Computation: Practice and Experience*, Vol. 34, No. 4, 2022, p. e6608.
- [18] Z. K. Şenturk, U. Süleyman, "An improved deep learning based cervical cancer detection using a median filter based pre-processing", *Avrupa Bilim ve Teknoloji Dergisi*, Vol. 32, 2022, pp. 50-58.
- [19] M. Zhao, H. Wang, Y. Han, X. Wang, H. N. Dai, X. Sun, J. Zhang, M. Pedersen, "Seens: Nuclei segmentation in pap smear images with selective edge enhancement", *Future Generation Computer Systems*, Vol. 114, 2021, pp. 185-194.
- [20] A. Khamparia, D. Gupta, V. H. C. de Albuquerque, A. K. Sangaiah, R. H. Jhaveri, "Internet of health things-driven deep learning system for detection and classification of cervical cells using transfer learning", *The Journal of Supercomputing*, Vol. 76, 2020, pp. 8590-8608.
- [21] A. Desiani, B. Suprihatin, S. Yahdin, A. I. Putri, F. R. Husein, "Bi-path Architecture of CNN Segmentation and Classification Method for Cervical Cancer Disorders Based on Pap-smear Images", *IAENG International Journal of Computer Science*, Vol. 48, No. 3, 2021.
- [22] O. Yaman, T. Tuncer, "Exemplar pyramid deep feature extraction based cervical cancer image classification model using pap-smear images", *Biomed-*

- ical Signal Processing and Control, Vol. 73, 2022, p. 103428.
- [23] N. D. Diniz et al. "A deep learning ensemble method to assist cytopathologists in pap test image classification", *Journal of Imaging*, Vol. 7, No. 7, 2021, p. 111.
- [24] H. Alquran, M. Alsalatie, W. A. Mustafa, R. A. Abdi, A. R. Ismail, "Cervical Net: A Novel Cervical Cancer Classification Using Feature Fusion", *Bioengineering*, Vol. 9, No. 10, 2022, p. 578.
- [25] K. P. Win, Y. Kitjaidure, K. Hamamoto, T. Myo Aung, "Computer-assisted screening for cervical cancer using digital image processing of pap smear images", *Applied Sciences*, Vol. 10, No. 5, 2020, p. 1800.
- [26] E. Hussain, L. B. Mahanta, C. R. Das, M. Choudhury, M. Chowdhury, "A shape context fully convolutional neural network for segmentation and classification of cervical nuclei in Pap smear images", *Artificial Intelligence in Medicine*, Vol. 107, 2020, p. 101897.
- [27] A. R. Bhatt, A. Ganatra, K. Kotecha, "Cervical cancer detection in pap smear whole slide images using convnet with transfer learning and progressive resizing", *PeerJ Computer Science*, Vol. 7, 2021, p. e348.
- [28] S. Dhawan, K. Singh, M. Arora, "Cervix image classification for prognosis of cervical cancer using deep neural network with transfer learning", *EAI Endorsed Transactions on Pervasive Health and Technology*, Vol. 7, No. 27, 2021.
- [29] P. V. Mulmule, R. D. Kanphade, "Supervised classification approach for cervical cancer detection using Pap smear images", *International Journal of Medical Engineering and Informatics*, Vol. 14, No. 4, 2022, pp. 358-368.
- [30] H. Alquran, W. A. Mustafa, I. A. Qasmieh, Y. M. Yacob, M. Alsalatie, Y. Al-Issa, A.M. Alqudah, "Cervical cancer classification using combined machine learning and deep learning approach", *Computers, Materials and Continua*, Vol. 72, No. 3, 2022, pp. 5117-5134.